Composites Science and Technology 241 (2023) 110148

Contents lists available at ScienceDirect

Composites Science and Technology

journal homepage: www.elsevier.com/locate/compscitech

Novel zone-based hybrid laminate structures for high-velocity impact (HVI) in carbon fibre-reinforced polymer (CFRP) composites

M.Erfan Kazemi [a,*], Victor Medeau [a], Lorenzo Mencattelli [a], Emile Greenhalgh [a], Paul Robinson [a], James Finlayson [b], Silvestre T. Pinho [a]

[a] Department of Aeronautics, Imperial College London, Exhibition Rd, South Kensington, London, SW7 2AZ, UK
[b] Composites - Structural Systems Design, Rolls-Royce, PO Box 31, Derby, DE24 8BJ, UK

A R T I C L E I N F O

Handling Editor: Marino Quaresimin

Keywords:
Carbon fibre-reinforced polymer (CFRP)
High-velocity impact (HVI)
Hybrid laminate
Damage tolerance
Thin-ply

A B S T R A C T

We propose novel zone-based hybrid laminate concepts for improving the high-velocity impact (HVI) response of baseline carbon fibre-reinforced polymer (CFRP) composites while maintaining similar areal weights and retaining substantial in-plane mechanical properties by requiring that about 80% (by mass) of the baseline CFRP is kept in the hybrid concepts. We identify three zones along the thickness of the laminate according to their role during HVI and implemented tailored materials in these zones to improve the HVI response. We studied a wide range of materials, including: fibre reinforcements of carbon (thin- and thick-plies), glass, Zylon and ultra-high molecular weight polyethylene (UHMWPE); a shape memory alloy/carbon fabric; and ceramic, alumina and titanium sheets. All laminate concepts have similar areal weights for a meaningful comparison. After defining the various concepts, we manufactured and measured their specific dissipated energy under HVI, and finally carried out post-mortem analysis (including C-scan and microscopy). The results show up to 95% improvement in energy dissipation over the baseline quasi-isotropic (QI) CFRP configuration.

1. Introduction

The application of carbon fibre-reinforced polymer (CFRP) laminates is of growing interest in multiple industries, namely aeronautics, due to their high-performance-to-weight ratio [1]. In terms of manufacturing, CFRP laminates have traditionally been made using conventional (thick-ply) prepregs. However, thin-ply CFRP prepregs are being increasingly considered as well. Thin-ply CFRPs can provide high resistance to matrix cracking and delamination while keeping in-plane mechanical properties equivalent to those of thick-ply CFRPs [2–4]. In addition, using thin-ply CFRPs increases the design space due to their lower thickness, thus providing a greater flexibility in the use of different materials and in tailoring the microstructure of the laminate accordingly.

Due to their brittle nature, CFRP laminates are susceptible to damage in various loading scenarios, especially in out-of-plane loading, including low-velocity impact (LVI) (such as tools drop during maintenance) and high-velocity impact (HVI) (such as birds strike during take-off and landing) [5,6]. To alleviate such a drawback, CFRP laminates have been successfully hybridised with different impact-resistant materials [7].

The main damage mechanisms in LVI include fibre breakage/failure, delamination and matrix cracking, and the response is mainly plate-bending dominated [7–9]. In contrast, in HVI events, the behaviour is longitudinal-wave dominated, and damage mechanisms are significantly more complex and localized (since the damage is created before the longitudinal waves reach the boundaries of the structure) [10]. Probably in part due to these complexities, HVI has received considerably less attention than LVI in the literature.

Wagner et al. [11] investigated the HVI response of hybrid laminates made of CFRP and glass fibre-reinforced polymer (GFRP) with similar thicknesses. They demonstrated that GFRPs show superior HVI performance compared to CFRP laminates of the same thickness. Tirillò et al. [12] hybridised CFRP laminates with basalt fibres with different stacking sequences and also compared them to a baseline CFRP laminate of similar thickness. They found that the HVI response of the hybrid laminates was superior to that of the CFRP baseline of the same thickness.

It is worth noting that GFRPs and Basalt fibres increase the weight of the laminate and reduce stiffness and strength (compared to a CFRP laminate with the same thickness). Therefore, there is value in

* Corresponding author.
E-mail address: m.kazemi@imperial.ac.uk (M.Erfan Kazemi).

https://doi.org/10.1016/j.compscitech.2023.110148
Received 10 February 2023; Received in revised form 18 May 2023; Accepted 5 July 2023
Available online 8 July 2023

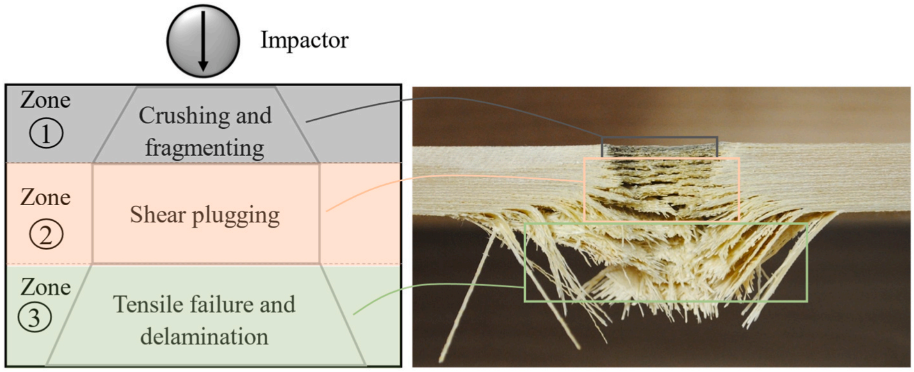

Fig. 1. Different zones TTT of a laminate subject to HVI; schematic on the left, and micrograph from Ref. [15] on the right.

additionally making comparisons with equivalent areal weight.

Li et al. [13] studied the role of carbon fibre and ultra-high molecular weight polyethylene (UHMWPE) fibre (Dyneema) on the HVI response of hybrid titanium-based fibre metal laminates (FMLs), for the same laminate aerial weight. They found that their FML with a combination of UHMWPE plies and titanium sheets had a higher ballistic performance than that of the carbon-based FML. Their FML with UHMWPE plies had no CFRP, hence the improvement in ballistic performance came at a significant stiffness and strength penalty.

In CFRP laminates subject to HVI, compressive stress waves are generated from the impact zone and travel through the thickness (TTT) of the laminate at the speed corresponding to the wave propagation velocity of the material [14]. These compressive waves then reach the rear side of the laminate and then return as tensile waves. In addition to TTT compressive waves, in-plane Lamb tensile waves travel towards the edge of the laminate [14].

The behaviour of a fibre-reinforced polymer (FRP) laminate under HVI can be usually categorized into three different zones [15] (Fig. 1):

1 Zone 1: crushing and fragmentation. In zone 1 (near the impact point, Fig. 1), crushing and fragmentation happen, which are mainly related to the TTT compression created near the impact point. To resist this, materials in this zone should exhibit high stiffness, the ability to redistribute stresses and to fragment [14]. Martinez-Hergueta et al. [15]investigated the HVI response of glass- and carbon-based FRPs with ceramics at the top and compared the response. They found that having ceramics at the impact side erodes the projectile, induces large plate bending, redistributes the load, and protects the first layers of underlying FRPs from being damaged. Other studies showed that by increasing the thickness of a ceramic layer, the ballistic limit of the laminates can be further improved [16, 17];
2 Zone 2: shear plugging. In zone 2 (towards the centre of the laminate, Fig. 1), shear plugging usually occurs, which corresponds to TTT shear failure and causes localized damage to appear around the periphery of the projectile. The dissipated energy is particularly low in this zone as the damage is confined to a small area; and
3 Zone 3: tensile failure and delamination. In zone 3 (located near the distal side of the laminate, Fig. 1) tensile failure and delamination happen. The higher the failure strain and ductility in this zone, the higher the dissipated energy.

Studies in the literature show that the structural integrity of CFRP laminates can be greatly improved when they are hybridised with various materials that provide (pseudo-)ductility in zone 3 and hence improve ballistic performance.

Hybridisation of CFRPs with high strain to failure fibres such as thin-ply PBO (Zylon) for containment casing applications can achieve this goal [18]; PBO fibres provide a higher tensile failure strain than that of carbon fibres and thus improve the tensile response at the rear side of the laminate. In addition, PBO fibres are lighter than Kevlar and exhibit higher intrinsic toughness which can further enhance ballistic performance [19]. High elongation at break and high modulus for better in-plane properties than Kevlar or Dyneema make PBO fibres a good option for hybridising CFRP laminates in zone 3 [18].

Table 1
Material families used for each zone in different FRP laminate concepts.

Material	Desired characteristics	Thick-ply family	Thin-ply family
Zone 1	High stiffness, load redistribution, fragmentation	Ceramic	D3O, Ceramic
Zone 2	Delaying shear plugging, delamination, diffusing failure	QI Aerospace-grade carbon-epoxy system	QI Skyflex
Zone 3	Delamination, high strain to failure	Titanium; PBO	GFRP; Dyneema; PBO; Carbon/SMA; Titanium

Various other materials can also achieve a similar purpose, namely UHMWPE (Dyneema) [20,21], titanium [22,23], woven carbon/shape memory alloy wires fabric [24] and GFRP [14].

We can conclude that, while much is understood about the potential of hybridisation for improving HVI of CFRP laminates, no study has shown whether any hybridising materials and corresponding hybridisation strategy can provide an improvement in HVI performance while not increasing mass, retaining substantial in-plane properties, and retaining the bulk of the baseline laminate. This is however a problem of fundamental industrial interest, in which there is an economical usage-phase cost related to added mass, there are in-plane loads that must be resisted, and the impact-prone region of a component must retain material continuity to the rest of that component.

In this study, we propose novel zone-based hybrid CFRP laminate concepts with improved HVI performance while keeping similar areal weights and retaining substantial in-plane mechanical properties by requiring that about 80% (by mass) of the baseline CFRP is kept in the hybrid concepts. In our investigation, we considered a particularly comprehensive range of hybridising materials, including various fibre reinforcements, metal alloys, ceramics, and a shape memory alloy, for both thin- and thick-ply CFRP baselines.

2. Methodology

2.1. Material selection and laminate concepts

We selected suitable materials to enhance the energy dissipation mechanisms in the zones identified in Fig. 1, both for thin- and thick-plies CFRP baseline laminate concepts (Table 1):

Table 2
Constituents, physical form and manufacturing details for the materials used.

Material	Fibre/resin type	Details	Manufacturing
Thin-ply (Skyflex USN20A)	TR50S/Epoxy K51	Unidirectional, 20 gsm (prepreg), 0.03 mm thick	Autoclave: 125 °C, 5 bar
Thick-ply	Aerospace-grade carbon-epoxy system (confidential)	Unidirectional, 268 gsm (prepreg), 0.25 mm thick	Confidential (information withheld by the sponsor)
GFRP (Hexply F155)	S-Glass: 4H satin/ Epoxy F155	Count (warp/fill – 60/ 58), 115 gsm, (prepreg)	Co-cured with SkyFlex
Dyneema HB26	UHMWPE/ Polyurethane matrix	0/90/0/90 unidirectionally-assembled prepreg	Hot pressed at 125 °C, 165 bar; then laid up with Skyflex prepreg
PBO	Zylon-HM545T/ TP513	Unidirectional, 25 gsm (prepreg)	Co-cured with Skyflex
Carbon/ SMA	Dry fabric 5H satin with SMA wires	Confidential, ~0.45 mm thick	The dry fabric is impregnated during curing with the excess resin
D3O – Hytrel	Not applicable	A closed-cell 2 mm thick polyurethane foam	Room temperature (3M scotch-weld EC-9323 b/a)
Alumina 96% tiles	Not applicable	0.5 mm thick from Precision Ceramics	Room temperature (3M scotch-weld EC-9323 b/a)
Titanium foil	Not applicable	ASTM B265 grade 2 titanium foil, 0.5 mm thick (no surface treatment)	Epoxy resin film to bond neighbouring titanium sheets

1. In zone 1, based on literature [15] and our preliminary studies, we considered ceramics for both thin- and thick-ply CFRPs. In addition, we selected D3O (a lightweight non-Newtonian foam for impact applications and an excellent shock absorber); it serves a similar function as a top ceramic layer but with 1/3 of its density, and is highly capable of redistributing stresses and absorbing shock waves [25];
2. In zone 2, we used quasi-isotropic (QI) CFRP to retain the desired substantial specific in-plane stiffness and strength; and
3. In zone 3, as the material needs to be (pseudo-)ductile and to undergo large strain/deformations, we selected titanium sheets, PBO, GFRP, Dyneema, and woven carbon/shape memory alloy (SMA) fabrics.

Further details about the materials listed in Table 1 are included in Table 2. The constraints for the design are that:

- within the limitations imposed by the finite thickness of the materials used, about 80% (by mass) of the baseline CFRP is kept in the hybrid concepts, and
- each laminate concept has a target areal weight of 0.95 g/cm^2. Using these constraints, as well as the materials in Tables 1 and 2, we defined the laminate concepts shown in Table 3.

2.2. Manufacturing

After laying up (Table 3) and curing (Table 3) the laminate concepts, we cut panels with the dimensions of 100 mm × 150 mm using an abrasive water jet cutting machine. Following this, we performed C-scan analyses on the manufactured specimens to ensure that good manufacturing quality had been achieved. Fig. 2 shows cross-sections of all manufactured laminate concepts and Table 3 shows the actual mass ratio of CFRP and the actual area weight for each laminate concept.

2.3. Instrumentation and analysis

To perform HVI tests, we used a 25 mm gas gun firing a steel ball with a diameter of 14 mm and a mass of about 11.25 g embedded in a foam sabot. Based on previous work performed at the University of Oxford [26], we manufactured a HVI test rig with simply-supported boundary conditions, Fig. 3 (a) and (b). The specimens were supported on the test rig with 4 ball bearings of 20 mm diameter, which were separated from each other by 100 mm, Fig. 3 (a). We used rubber bands to hold the specimens on the test rig, Fig. 3 (c) and (d). The low modulus and strength of these rubber bands can safely ignore the constraints imposed by them [26]. For each laminate concept, we tested different samples at 170 m/s and 210 m/s, both above the ballistic limit of the thin-ply CFRP specimen (measured ~130 m/s) and thick-ply CFRP specimen

Table 3
Layups configuration and properties of the laminate concepts.

	Laminate concept name	Zone 1	Zone 2	Zone 3	Layup	Thickness (mm)	Actual mass ratio of CFRP	Actual areal weight (g /cm^2)	Laminate concept code
Thin-ply family	Thin-ply/Cer	Ceramic	QI Skyflex	–	Alu, $(60_c/0_c/\text{-}60_c)_{65}$	5.3	0.80	0.94	i
	Thin-ply/GFRP	–	QI Skyflex	GFRP	$(60_c/0_c/\text{-}60_c)_{63}$, G_{10}	5.0	0.83	0.79	ii
	QI Thin-ply	–	QI Skyflex	–	$[(60_c$[a]$/0_c/\text{-}60_c)_{40}, 0_{1/2}]_s$[b]	5.5	1.00	0.84	iii
	Thin-ply/D3O	D3O	QI Skyflex	–	D3O, $(60_c/0_c/\text{-}60_c)_{61}$	7.2	0.76	0.87	iv
	Thin-ply/SMA	–	QI Skyflex	Carbon/ SMA	CFRP[c]$_{35}$, CS, CFRP$_5$, CS, CFRP$_5$, CS, CFRP$_5$, CS, CFRP$_5$	5.0	0.65	0.90	v
	Thin-ply/Ti	–	QI Skyflex	Titanium	$(60_c/0_c/\text{-}60_c)_{62}$, $(Ti)_{10}$	4.8	0.75	0.86	vi
	Thin-ply/PBO	–	QI Skyflex	PBO	$(60_c/0_c/\text{-}60_c)_{62}$, $(60_z/0_z/\text{-}60_z)_{17}$	5.4	0.80	0.80	vii
	Thin-ply/Dyn	–	QI Skyflex	Dyneema	$(60_c/0_c/\text{-}60_c)_{63}$, $((0_d/90_d)_2)_8$	6.4	0.79	0.84	viii
Thick-ply family	Thick-ply/Cer	Ceramic	QI C/Ep	–	Alu, $(60_c/0_c/\text{-}60_c)_6$	5.3	0.75	0.88	ix
	QI Thick-ply	–	QI C/ Ep[d]	–	$(60_c/0_c/\text{-}60_c)_{4S}$	6.4	1.00	0.94	x
	Thick-ply/Ti	–	QI C/Ep	Titanium	$(60_c/0_c/\text{-}60_c)_6$, $(Ti)_{10}$	5.1	0.75	0.94	xi

[a] c: carbon, z: Zylon (PBO), d: Dyneema, CS: carbon/SMA.
[b] $[(60_c/0_c/\text{-}60_c)_{40}, 0_{1/2}]_s$: $(60_c/0_c/\text{-}60_c)_{40}$ + single 0_c layer + $(60_c/0_c/\text{-}60_c)_{40}$.
[c] CFRP: Thin-ply $[60_c/0_c/\text{-}60_c]$.
[d] C/Ep: confidential Aerospace-grade carbon-epoxy system.

Fig. 2. Cross-sections of manufactured thin- and thick-ply laminate concepts (scaled).

(measured ~150 m/s), which serve as baselines for this study. To track the impact event and calculate the impact and residual velocities, we used two high-speed cameras in the test setup, Fig. 3 (c) and (d).

3. Results

Fig. 4 (a) and (c) show normalised specific energy dissipated by the thin and thick-ply laminate concepts respectively. We calculated the dissipated energy of all the impacted thin- and thick-ply laminate concepts and normalised those values with respect to the dissipated energy of the QI thin-ply baseline impacted at 170 m/s.

Fig. 4 (b) and (d) show the respective average variation over the corresponding QI baselines. As in each of the laminate concept designs, both of the specimens perforated at 170 and 210 m/s (except Thin-ply/Dyn), we used mean values to provide the range of specific dissipated energy, where perforation occurred.

Fig. 4 (e) and (f) compare specifically the average energy dissipated by each thin-ply CFRP laminate concept to the respective thick-ply concept.

Fig. 5 and Fig. 6 show C-scans, highlighting the delaminations, as well as photographs of the impact and distal sides, for thin- and thick-ply laminate concepts respectively.

Fig. 7 (a–h) and Fig. 7 (i-k) show cross-sections of impacted specimens for each thin- and thick-ply laminate concept respectively. Fig. 8 presents a higher-magnification comparison of the baseline monolithic thin- and thick-ply specimens.

4. Discussion

4.1. Role of hybrid material on HVI of thin-ply CFRPs

Fig. 4 (a) and (b) show that hybridising the thin-ply baseline with ceramic, D3O or GFRP did not improve energy dissipation compared to the baseline, while hybridising the baseline with Dyneema, PBO or titanium remarkably increased the energy dissipation up to 95%, 88%, and 31%, respectively. On average, we achieved a wide range of improvements in energy dissipation (considering both velocities) over the average energy dissipation of the monolithic thin-ply CFRP baseline: up to 31% for thin-ply/titanium, 73% for thin-ply/PBO, and 74% for thin-ply/Dyneema. Regarding each of the thin-ply hybrid laminate concepts:

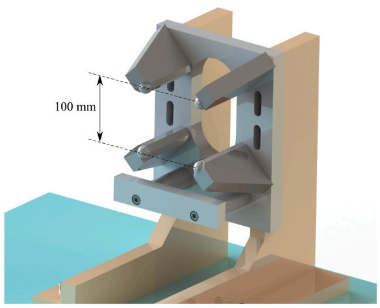

(a) Schematic of the Oxford HVI test rig [26]

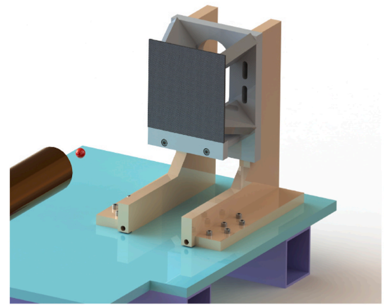

(b) Schematic of the full Oxford HVI test setup [26]

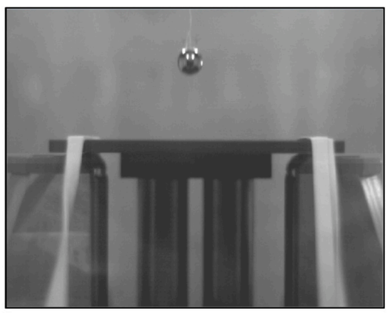

(c) Side view of HVI test

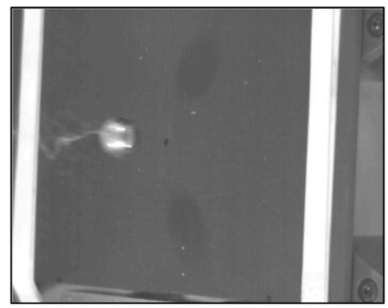

(d) Top view of HVI test

Fig. 3. HVI test configuration (see video of the test as separate artwork).

- applying ceramic on the impact side results in fragmentation of the ceramic sheet under the impactor, Fig. 5 (a); however, we did not observe radial cracks in the ceramic layer (as detected in the literature for thicker layers of ceramic [15]), suggesting the absence of redistribution of stresses in the underlying thin-ply CFRP plies. In this laminate concept, we measured lower energy dissipation than that of the baseline, which confirms that this laminate concept not only does not promote delamination or increase the damaged area compared to that of the baseline, but also reduces specific energy dissipation;
- by introducing GFRPs on the distal side, we detected large diamond-shaped delaminations at the GFRP/CFRP interface, Fig. 5 (b). However, we did not witness delaminations inside the CFRP block, and as a consequence, we did not achieve improvements in the specific energy dissipation (Fig. 4 (a)), which might be due to the lower thickness of the sample and the limited number of GFRP layers applied to this laminate concept. It should be noted that, in this study, we required that about 80% (by mass) of the baseline CFRP be kept in the hybrid concepts (so this lack of improvement does not necessarily generalise for larger fractions of GFRP);
- regarding the thin-ply baseline, delamination stays confined to the vicinity of the impactor (Fig. 5 (c)). In addition, the damage is brittle and does not extend much, and failure is seemingly confined under the impactor area;
- by placing a D3O foam layer on the impact side, we observed an approximately 11% increase in the average specific energy dissipation, Fig. 4 (b). In addition, we identified a wider shear plug diameter in the failed specimen compared to that of both the baseline and thin-ply/ceramic laminate concept (Fig. 5 (d)), confirming the presence of stress redistribution in the D3O layer; a phenomenon that we did not observe in either the baseline, ceramic-based or GFRP hybrid laminate concepts. Furthermore, we detected a greater extent of damage at the distal side;
- by applying woven carbon/shape memory alloy (SMA) fabrics on the distal side, we detected dispersed delamination (Fig. 5 (e)), which is due to the presence of SMA wires in the laminate concept. When the SMA wires embedded inside the laminate concept were impacted, dispersed delamination between the wires and the surrounding CFRPs created, which is revealed as scattered blue parts in the C-scan, Fig. 5 (e). After perforation, the rear side of the laminate concept shows failed fibres and wires (of the SMA due to pull-out at the distal side). For this laminate concept, we obtained a slight increase in the dissipated energy over the baseline and thin-ply/D30, Fig. 4 (a) and (b). However, we did not observe greater delamination extent in this laminate concept due to the limited number of woven carbon/SMA fabrics used (only 4 plies);
- by inserting titanium foils on the distal side, we achieved a 22% increase at 170 m/s and a 27% increase at 210 m/s in energy dissipation over corresponding baselines, Fig. 4 (b). Important petalling and delamination at the thin-ply/titanium interface occurred; however, delamination detection in the CFRP layer was made difficult due to the presence of the titanium layers, Fig. 5 (f);
- by applying PBO prepregs on the distal side, we achieved the strongest improvement over the baseline with a 88% and 62% increase in specific energy dissipation at 170 and 210 m/s, respectively (with an average of 73% improvement compared to that of the QI thin-ply baseline, Fig. 4 (a) and (b)). This significant improvement is related to: (1) the high strain to failure of Zylon (PBO) fibres, which provide significant resistance and energy dissipation in impact [27, 28]; and (2) the very low thickness of PBO plies, which let the laminate concept contain many plies in a limited thickness (51 plies), which promoted delamination and thus energy dissipation during HVI. Delamination at the rear side of thin-ply/PBO extends to the edges of the laminate. We did not observe significant delamination inside the CFRP block, Fig. 5 (g); and
- in all thin-ply laminate concepts except for thin-ply/Dyneema, the hybridising layer(s) stay in place after impact, and full perforation with partial or complete delamination of the distal layer(s) occurs, Fig. 5. However, in the thin-ply/Dyneema laminate concept, the Dyneema block debonds and flies away with the projectile after

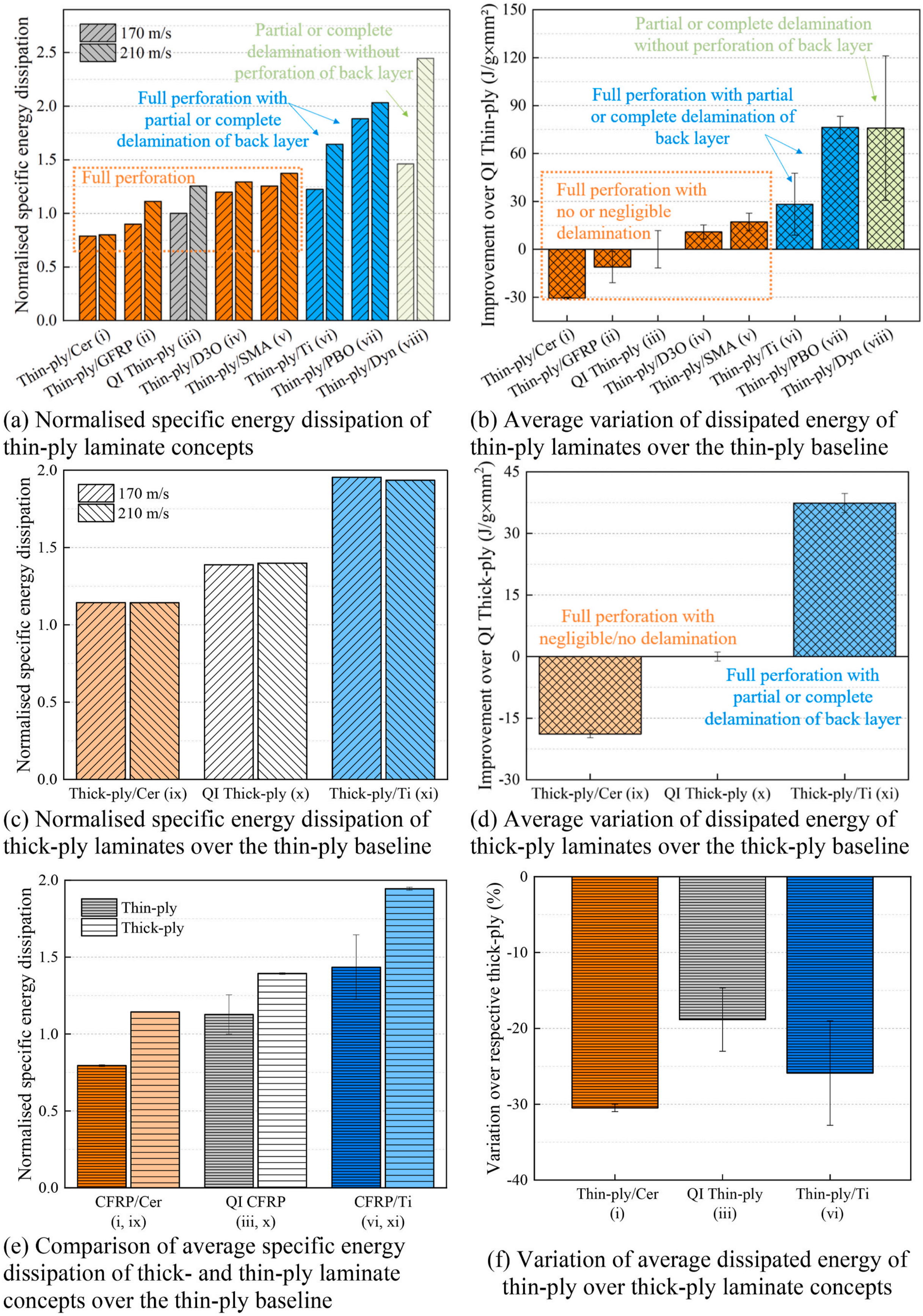

Fig. 4. Specific energy dissipation of thin- and thick-ply CFRP laminate concepts and their average variations over baselines.

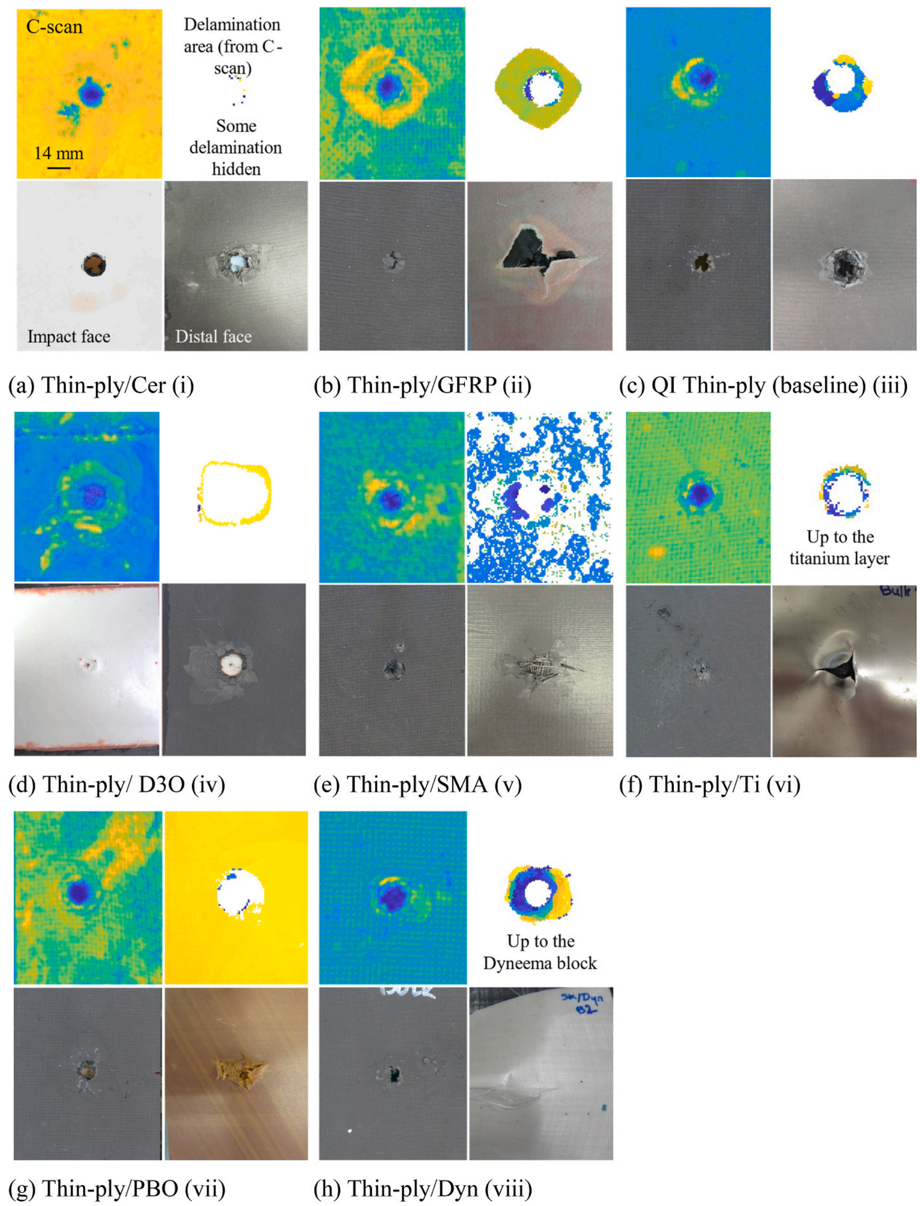

Fig. 5. Post-mortem (consisting of C-scan, delamination, impact and distal) images of thin-ply laminate concepts impacted at 210 m/s.

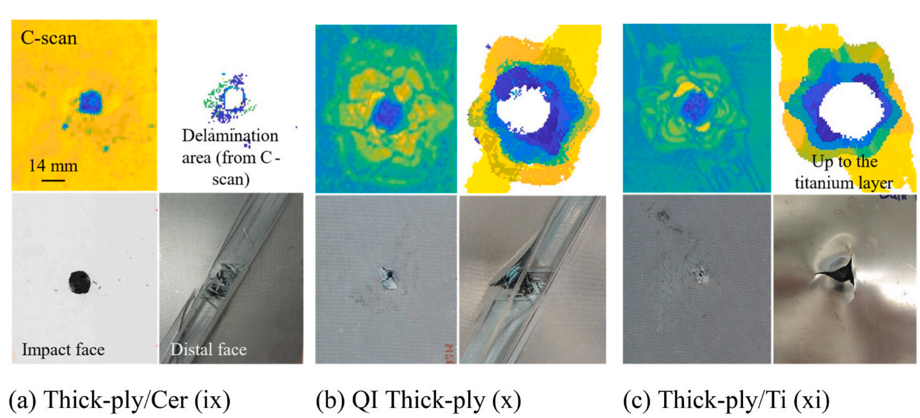

Fig. 6. Post-mortem (consisting of C-scan, delamination, impact and distal) images of thick-ply laminate concepts impacted at 210 m/s.

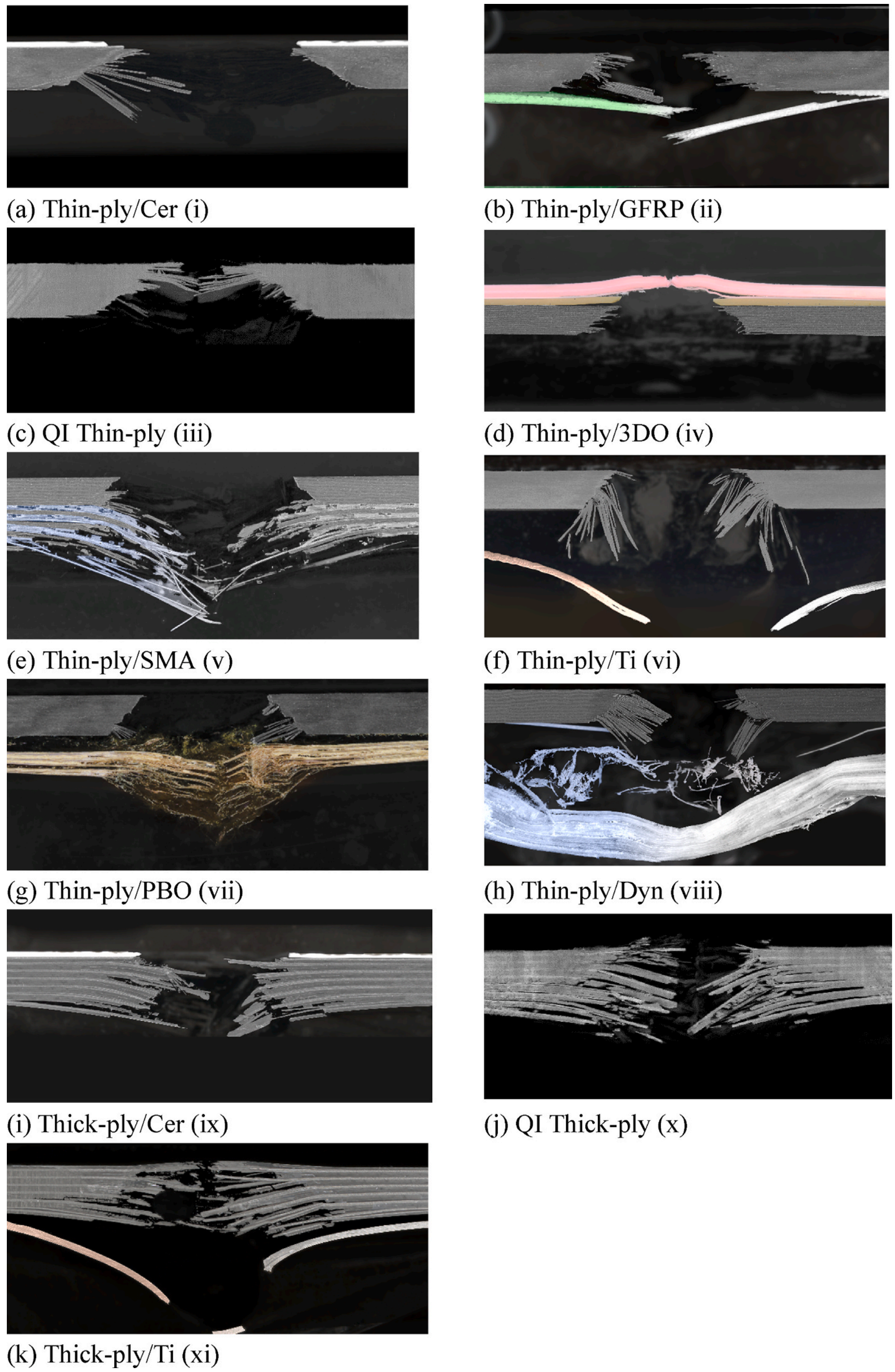

Fig. 7. Cross-sections of hybrid thin and thick-ply laminate concepts impacted at 210 m/s.

impact (due to the inherently poor interfacial properties of UHMWPE fibres with other fibre reinforcements and other resin systems [29]), Fig. 5 (h). As a result, the obtained specific dissipated energy value for thin-ply/Dyneema should not be directly compared to other laminate concepts. Shanmugam et al. [30] showed that we could potentially have achieved a stronger improvement by applying an appropriate surface treatment. During the impact test of thin-ply/Dyneema, we noticed the projectile deflected and exited on the lateral side or flew off with the Dyneema block. Hence, full delamination of the Dyneema layer without perforation happened. This implies that the improvement of 95% (at 210 m/s) should not be directly compared against the improvement for the other laminate concepts.

4.2. Role of hybrid material on HVI of thick-ply CFRPs

In terms of specific energy dissipation and improvement for thick-ply laminate concepts, the results show a similar trend compared to the results of thin-ply laminate concepts, Fig. 4 (c) and (d). In this regard, adding a ceramic layer on the impact side of the thick-ply CFRP baseline did not improve the response, while applying titanium foils on the distal side enhanced the specific energy dissipation by more than 40% compared to that of the thick-ply baseline. This improvement is higher

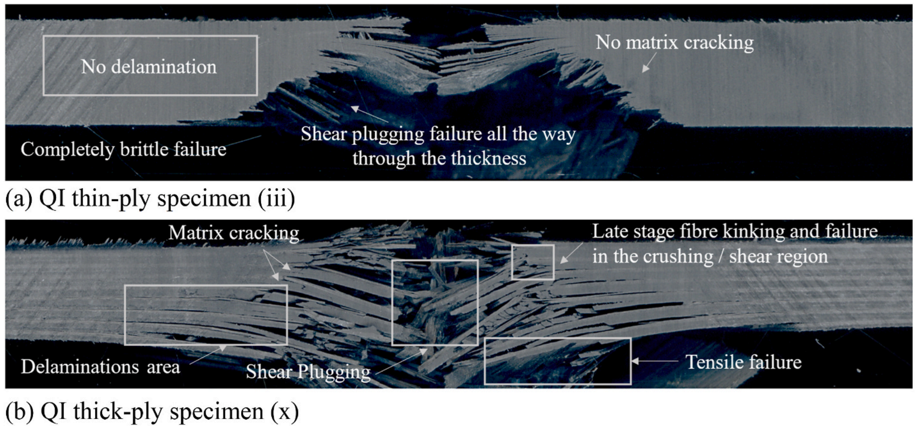

Fig. 8. Cross-sections of monolithic QI (a) thin- and (b) thick-ply baselines impacted at 210 m/s.

than that obtained for the thin-ply/Ti laminate concept specimens, which is related to the difference in mechanical properties between the thin- and thick-plies, since both laminate concepts have almost similar areal weight and hybridising ratio.

Compared to their thin-ply counterparts, the thick-ply laminate concepts underwent more extensive delamination, which increased in size toward the distal side, Fig. 6 (b). In addition, we observed spalling at the distal side of all thick-ply laminate concepts: a failure that we did not detect in thin-ply laminate concepts, and which contributes to higher energy dissipation, Fig. 6. Post-mortem impact-side and distal-side photographs of a thick-ply/ceramic specimen show that the ceramic layer fragmented over an area corresponding to the size of the projectile, Fig. 6 (a). However, similar to the behaviour of the thin-ply/Cer laminate concept, we did not observe any further damage in the ceramic layer, resulting in lower energy dissipation than that of the thick-ply baseline, Fig. 4 (d). Nonetheless, spalling of carbon fibres still occurred on the distal side, Fig. 6 (a). Concerning the HVI response of thick-ply/titanium, we notice an important petalling and delamination at the titanium/CFRP interface with a delamination area similar to that of the thick-ply baseline, Fig. 6 (c).

4.3. *Thick-ply vs. thin-ply CFRP*

By comparing the behaviour of monolithic QI thin- and thick-ply specimens provided in Fig. 4 (e, middle columns) we found that the thick-ply baseline (either at 170 or 210 m/s) dissipated about 39% more energy compared to the QI thin-ply baseline impacted at 170 m/s. This shows an average of about 24% higher in dissipated energy (considering both velocities) compared to the average energy dissipation of the thin-ply counterpart. However, it should be noted that the thick-ply laminate comes with a slightly higher thickness and areal weight (Table 3). In any case, the main reason for lower energy dissipation of the thin-ply baseline may more likely be attributed to a lower translaminar fracture toughness and to a smaller delamination for a similar layup. We observed a similar trend for the rest of the hybrid laminate concepts, showing that hybrid thin-ply laminate concepts dissipated around 20% lower energy compared to their thick-ply counterparts, Fig. 4 (f).

Cross-section analyses (Fig. 7) show that applying ceramic (Fig. 7 (a) and (i)) or GFRP (Fig. 7 (b)) did not change the failure mechanisms of the developed laminate concepts compared to that of the baselines, (Fig. 7 (c) and (j)), since the low thickness of introduced hybrid material was not enough to trigger a change in failure mechanisms. However, applying (pseudo-)ductile materials (Fig. 7 (d-h) and (k)) resulted in delayed tensile failure at the distal side, allowing for more energy dissipation.

Failure analysis of the cross-sections of monolithic thin- and thick-ply baselines shows that the thin-ply baseline failed in a brittle way, mainly due to the prevalent shear plugging mechanism, Fig. 8 (a). Moreover, the damage is confined around the projectile path, and thus, we did not witness any significant delamination or matrix cracking away from the impact zone. This behaviour accounted for the lower energy dissipated by this specimen since shear plugging has been reported to be a minor energy dissipation mechanism [31]. By contrast, the thick-ply baseline exhibited more complex failure mechanisms (Fig. 8 (b)), including extended delaminations, matrix cracking, and late-stage fibre kinking away from the projectile path. Plies at the rear side of the thick-ply specimen appear to have failed in tension rather than shear plugging, contributing to higher energy dissipation.

5. Conclusions

In this paper, we developed various novel zone-based hybrid CFRP laminate concepts with improved HVI performance while keeping similar areal weights and retaining substantial in-plane mechanical properties by requiring that 80% (by mass) of the baseline CFRP is kept in the hybrid concepts. We designed and manufactured hybrid laminate concepts (with baseline thin-ply [Skyflex] or thick-ply CFRPs) using a range of hybridising materials – namely glass, Zylon [PBO] and UHMWPE [Dyneema] prepregs, titanium foils, ceramic sheets, and carbon fibre/shape memory alloy fabrics. We then tested specimens at 170 m/s and 210 m/s, and analysed each laminate concept in terms of their specific dissipated energy and related failure modes. We obtained a strong quantitative ranking for all of the laminate concepts and concluded that:

- among all the thin-ply CFRP concepts, the most promising ones are hybrids of (Skyflex-based) thin-ply/Dyneema, thin-ply/PBO and thin-ply/Titanium, with up to 95%, 88% and 31% improvements over the QI [60/0/-60] thin-ply baseline, respectively. Among the thick-ply CFRP concepts, the thick-ply/titanium concept performs best, with up to 40% improvement over the monolithic QI CFRP thick-ply baseline.
- post-mortem and fractographic analyses reveal that in QI thin-ply CFRP concepts, shear-plugging is the main failure mechanism, which only dissipates very limited energy; damage is confined around the projectile path and no delamination or matrix cracking was detected away from the impact zone. In contrast, thick-ply specimens exhibit more complex failure mechanisms with significant delamination, matrix cracking and late-stage fibre kinking away from the projectile path. Nonetheless, thin-ply CFRP can potentially provide a larger design-space of interleaved hybrids, with benefits which could compensate for the decrease in performance in our particular study; and

- some of the hybrid concepts, such as those with ceramic and GFRP, did not in our study improve the HVI performance over the baseline. This might be due to the low amount of these materials introduced into the hybrid laminate (in our case as a result of integrating a meaningful CFRP mass constraint into our concepts), which may not have been enough to trigger a change in failure mechanisms.

Credit authorship contribution statement

M.Erfan Kazemi: Methodology, Formal analysis, Investigation, Writing – original draft, Visualisation. **Victor Médeau:** Conceptualisation, Methodology, Investigation, Writing – review & editing. **Lorenzo Mencattelli:** Conceptualisation, Methodology, Investigation. **Emile Greenhalgh:** Resources, Supervision, Funding acquisition. **Paul Robinson:** Resources, Supervision, Funding acquisition. **James Finlayson:** Conceptualisation, Resources, Project administration. **Silvestre T. Pinho:** Conceptualisation, Methodology, Writing – review & editing, Supervision, Funding acquisition, Project administration.

Declaration of competing interest

The authors declare that they have no known competing financial interests or personal relationships that could have appeared to influence the work reported in this paper.

Data availability

The authors do not have permission to share data.

Acknowledgements

The funding from Innovate UK under the UKRI FANDANGO project No. 113232 (https://gtr.ukri.org/projects?ref=113232) is gratefully acknowledged.

Appendix A. Supplementary data

Supplementary data to this article can be found online at https://doi.org/10.1016/j.compscitech.2023.110148.

References

[1] C. Bouvet, Mechanics of Aeronautical Composite Materials, John Wiley & Sons, 2017.
[2] L. Mencattelli, S.T. Pinho, Ultra-thin-ply CFRP Bouligand bio-inspired structures with enhanced load-bearing capacity, delayed catastrophic failure and high energy dissipation capability, Compos. Appl. Sci. Manuf. 129 (2020), 105655.
[3] R. Amacher, J. Cugnoni, J. Botsis, L. Sorensen, W. Smith, C. Dransfeld, Thin ply composites: experimental characterization and modeling of size-effects, Compos. Sci. Technol. 101 (2014) 121–132.
[4] A. Wagih, P. Maimí, E.V. González, N. Blanco, J.R.S. de Aja, F.M. de la Escalera, et al., Damage sequence in thin-ply composite laminates under out-of-plane loading, Compos. Appl. Sci. Manuf. 87 (2016) 66–77.
[5] G.R. Villanueva, W. Cantwell, The high velocity impact response of composite and FML-reinforced sandwich structures, Compos. Sci. Technol. 64 (2004) 35–54.
[6] C. Vakili Rad, K. Kodagali, J. Roark, D. Revilock, C. Ruggeri, R. Harik, et al., High velocity impact response of hybridized pseudo-woven carbon fiber composite architectures, Compos. B Eng. 203 (2020), 108478.
[7] M.E. Kazemi, L. Shanmugam, A. Dadashi, M. Shakouri, D. Lu, Z. Du, et al., Investigating the roles of fiber, resin, and stacking sequence on the low-velocity impact response of novel hybrid thermoplastic composites, Compos. B Eng. 207 (2021), 108554.
[8] Y. Swolfs, Y. Geboes, L. Gorbatikh, S.T. Pinho, The importance of translaminar fracture toughness for the penetration impact behaviour of woven carbon/glass hybrid composites, Compos. Appl. Sci. Manuf. 103 (2017) 1–8.
[9] Z. Aslan, R. Karakuzu, B. Okutan, The response of laminated composite plates under low-velocity impact loading, Compos. Struct. 59 (2003) 119–127.
[10] W. Cantwell, J. Morton, Comparison of the low and high velocity impact response of CFRP, Composites 20 (1989) 545–551.
[11] T. Wagner, S. Heimbs, F. Franke, U. Burger, P. Middendorf, Experimental and numerical assessment of aerospace grade composites based on high-velocity impact experiments, Compos. Struct. 204 (2018) 142–152.
[12] J. Tirillò, L. Ferrante, F. Sarasini, L. Lampani, E. Barbero, S. Sánchez-Sáez, et al., High velocity impact behaviour of hybrid basalt-carbon/epoxy composites, Compos. Struct. 168 (2017) 305–312.
[13] X. Li, X. Zhang, Y. Guo, V.P.W. Shim, J. Yang, G.B. Chai, Influence of fiber type on the impact response of titanium-based fiber-metal laminates, Int. J. Impact Eng. 114 (2018) 32–42.
[14] R. Muñoz, F. Martínez-Hergueta, F. Gálvez, C. González, J. Llorca, Ballistic performance of hybrid 3D woven composites: experiments and simulations, Compos. Struct. 127 (2015) 141–151.
[15] F. Martinez-Hergueta, Multiscale FE Modelling and Design of Composite Laminates under Impact. Reference Module in Materials Science and Materials Engineering, 2018.
[16] I.C. Benloulo, V. Sanchez-Galvez, A new analytical model to simulate impact onto ceramic/composite armors, Int. J. Impact Eng. 21 (1998) 461–471.
[17] B. Tepeduzu, R. Karakuzu, Ballistic performance of ceramic/composite structures, Ceram. Int. 45 (2019) 1651–1660.
[18] M.J. Kappes, R.W. Heeter, B.N. Hodgson, Fan Containment Case for a Gas Turbine Engine, Google Patents, 2020.
[19] J.-M. Park, D.-S. Kim, S.-R. Kim, Improvement of interfacial adhesion and nondestructive damage evaluation for plasma-treated PBO and Kevlar fibers/epoxy composites using micromechanical techniques and surface wettability, J. Colloid Interface Sci. 264 (2003) 431–445.
[20] F. Zulkifli, J. Stolk, U. Heisserer, A.T.-M. Yong, Z. Li, X.M. Hu, Strategic positioning of carbon fiber layers in an UHMwPE ballistic hybrid composite panel, Int. J. Impact Eng. 129 (2019) 119–127.
[21] S. Heimbs, T. Wagner, Lozoya JT. Viana, B. Hoenisch, F. Franke, Comparison of impact behaviour of glass, carbon and Dyneema composites, Proc. IME C J. Mech. Eng. Sci. 233 (2019) 951–966.
[22] R. Häsä, S.T. Pinho, A three-level hybrid metal/in-plane-CFRP/crossed-lamellar microstructure concept for containment applications, Compos. Appl. Sci. Manuf. 126 (2019), 105609.
[23] M.E. Kazemi, M. Bodaghi, L. Shanmugam, M. Fotouhi, L. Yang, W. Zhang, et al., Developing thermoplastic hybrid titanium composite laminates (HTCLS) at room temperature: low-velocity impact analyses, Compos. Appl. Sci. Manuf. 149 (2021), 106552.
[24] A. Foreman, T. Nensi, C. Meeks, P. Curtis, An integrated system for improved damage resistance and lightning strike protection in composite structures, in: 16th International Conference on Composite Materials (Kyoto), 2007.
[25] A.A. Shargawi, Mechanical Testing and Evaluation of D3O® Material for Adequacy of an Ergonomic Intervention for Vibration Transmission Reduction in Aircraft Manufacturing, Wichita State University, 2020.
[26] H. Cui, D. Thomson, S. Eskandari, N. Petrinic, A critical study on impact damage simulation of IM7/8552 composite laminate plate, Int. J. Impact Eng. 127 (2019) 100–109.
[27] S. Zangana, J. Epaarachchi, W. Ferdous, J. Leng, A novel hybridised composite sandwich core with Glass, Kevlar and Zylon fibres – investigation under low-velocity impact, Int. J. Impact Eng. 137 (2020), 103430.
[28] M. Padhan, U. Marathe, J. Bijwe, Exceptional performance of bi-directionally reinforced composite of PEEK manufactured by commingling technique using poly (p-phenylene-benzobisoxazole) (PBO) fibers, Compos. Sci. Technol. 218 (2022), 109125.
[29] L. Shanmugam, X. Feng, J. Yang, Enhanced interphase between thermoplastic matrix and UHMWPE fiber sized with CNT-modified polydopamine coating, Compos. Sci. Technol. 174 (2019) 212–220.
[30] L. Shanmugam, M.E. Kazemi, Z. Li, W. Luo, Y. Xiang, L. Yang, et al., Low-velocity impact behavior of UHMWPE fabric/thermoplastic laminates with combined surface treatments of polydopamine and functionalized carbon nanotubes, Compos. Commun. 22 (2020), 100527.
[31] L. Alonso, F. Martínez-Hergueta, D. Garcia-Gonzalez, C. Navarro, S.K. García-Castillo, F. Teixeira-Dias, A finite element approach to model high-velocity impact on thin woven GFRP plates, Int. J. Impact Eng. 142 (2020), 103593.